Acta Pharmaceutica Sinica B 2012;2(2):137–145

Institute of Materia Medica, Chinese Academy of Medical Sciences
Chinese Pharmaceutical Association

Acta Pharmaceutica Sinica B

www.elsevier.com/locate/apsb
www.sciencedirect.com

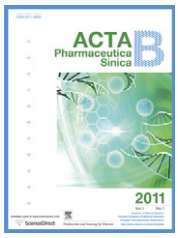

ORIGINAL ARTICLE

Cytochrome P450 2C24: expression, tissue distribution, high-throughput assay, and pharmacological inhibition

Jun Yang[a], Melissa A. VanAlstine[a,†], James G. Phillips[b], Mark P. Wentland[c], Lindsay B. Hough[a,*]

[a]*Center for Neuropharmacology and Neuroscience, Albany Medical College, Albany, NY 12208, USA*
[b]*Curragh Chemistries, Cleveland, OH 44106, USA*
[c]*Department of Chemistry, Department of Chemistry and Chemical Biology, Rensselaer Polytechnic Institute, Troy, NY 12180, USA*

Received 9 January 2012; revised 16 January 2012; accepted 12 February 2012

KEY WORDS

Cytochrome P450 2C24;
Cytochrome P450 2C55;
P450 inhibitors;
Brain;
Pain;
Analgesia

Abstract Cytochrome P450 (CYP)-mediated epoxidation of arachidonic acid (AA) contributes to important biological functions, including the pain-relieving responses produced by analgesic drugs. However, the relevant epoxygenase(s) remain unidentified. Presently, we describe the tissue distribution, high-throughput assay, and pharmacological characteristics of the rat epoxygenase CYP2C24. Following cloning from male rat liver, recombinant baculovirus containing the C-terminal His-tagged cDNA was constructed and used to express the protein in *Spodoptera frugiperda* (Sf9) cells. Enzymatic activity was detected with membranes, NADPH regenerating system and CYP reductase, and optimized for high throughput screening by use of the Vivid Blue© BOMCC fluorescence substrate. Quantitative real-time PCR identified CYP2C24 m-RNA in liver, kidney, heart, lung, gonad and brain. Screening of CYP2C24 activity against a panel of inhibitors showed a very strong correlation with activity against the human homologue CYP2C19. In agreement with recent findings on CYP2C19, the epoxygenase blockers PPOH and MS-PPOH inhibited CYP2C24 only weakly, confirming that these drugs are not universal epoxygenase inhibitors. Finally, comparisons of the CYP2C24 inhibitor profile with anti-analgesic activity suggests that this isoform does not contribute to brain analgesic drug action. The present methods and pharmacological data will aid in study of the biological significance of this CYP isoform.

*Corresponding author at: Center for Neuropharmacology and Neuroscience, Albany Medical College MC-136, 47 New Scotland Ave, Albany, NY 12208, USA. Tel.: +1 518 262 5786.
E-mail address: houghl@mail.amc.edu (Lindsay B. Hough).
†Present address: Chemistry Department, Adelphi Univ., 1 South Ave., Garden City, NY 11530, USA.

Peer review under responsibility of Institute of Materia Medica, Chinese Academy of Medical Sciences and Chinese Pharmaceutical Association.
doi:10.1016/j.apsb.2012.02.003

Production and hosting by Elsevier

1. Introduction

The metabolism of arachidonic acid (AA) by cyclooxygenases, lipoxygenases and/or epoxygenases leads to production of many mediators, including prostanoids, thromboxanes, leukotrienes, hepoxillins, hydroxyeicosatetraenoic acids (HETEs) and epoxyeicosatrienoic acids (EETs)[1]. Many cytochrome P450 monooxygenases (CYPs) participate in these pathways by catalyzing AA hydroxylation and/or epoxidation to produce HETEs and EETs[2]. CYP-derived eicosanoids are thought to perform a variety of important biological functions, including regulation of ion transport, cellular proliferation, apoptosis, inflammation, and hemostasis[3]. More recent studies have implicated AA epoxygenase products in other functions, including vascular regulation[4,5], neurovascular dilation[6], and analgesic drug action[7–9]. However, many of the biologically relevant epoxygenases have not been identified, especially in the brain.

Members of several CYP subfamilies can perform AA epoxidation, including CYP1A, CYP2B, CYP2C, CYP2D, CYP2E, CYP2N, CYP2G, CYP2J, CYP4A and CYP4X[10–16]. Of these, the CYP2C subfamily is the largest[17], yet information is lacking on many CYP2C isoforms. CYP2C24, a rat CYP2C isoform cloned in 1991[18,19] is closely related to rat CYP2C11 (75% homology), rat CYP2C6 (72%), human CYP2C18 (78%) and human CYP2C19 (74%). Although CYP2C24 was reported to be the second-most abundant CYP2C isoform in the kidney[17], little is known about this particular isoform. CYP2C24 was detected by Northern analysisin rat kidney, liver and prostate[19], but the existence of this enzyme in other tissues is not known. Recombinant CYP2C24 was reported to catalyze AA metabolism to mixtures of epoxy- and monohydroxylated acids, implying an epoxygenase role for this enzyme[20]. However, we are unaware of any other information on substrates, inhibitors, or methodologies for the study of this enzyme. Presently, we demonstrate the existence of CYP2C24 in the rat brain, describe the development of a high-throughput screening method utilizing baculovirus-expressed enzyme, and report the effects of inhibitors on this enzyme.

2. Materials and methods

2.1. Materials

7-Dimethylamino-4-trifluoromethylcoumarin (C152), 4-, 4'-biphenylaldehyde (4-BA), 7-ethoxy-4-trifluoromethylcoumarin (EFC), Vivid© BOMCC substrate (3-cyano-7-(benzyloxymethoxy)-coumarin), and Vivid Blue© fluorescent standard (3-cyano-7-hydroxy-coumarin) were purchased from Invitrogen (Carlsbad, CA). Methoxy-4-trifluoromethylcoumarin (MFC), 7-hydroxy-4-trifluoromethylcoumarin, dibenzylfluorescein (DBF) and cDNA-expressed P450s (CYP2C8, CYP2C9) were purchased from BD Bioscience (Woburn, MA). Acetonitrile (HPLC grade) and magnesium chloride hexahydrate were purchased from Fisher Scientific (Pittsburgh, PA). Sulconazole, quercetin and ticlopidine were purchased from Krackeler Scientific, Inc. (Albany, NY). Miconazole and fluconazole were purchased from MP Bioscience (Buxton, UK). *N*-(Methylsulfonyl)-2-(2-propynyloxy)-benzenehexanamide (MS-PPOH) and 2-(2-propynyloxy)-benzenehexanoic acid (PPOH) were purchased from Cayman Chemicals (Ann Arbor, MI). CC12 [4(5)-((4-iodobenzyl)thiomethyl)-1*H*-imidazole[21]] and MW06-25 [*N*-((4-iodobenzyl)thiomethyl)-imidazole[8]] were available from laboratory stock. Enzyme assays were conducted in black Costar 96-well plates (Corning Incorporated, Corning, NY). All other reagents were purchases from Sigma-Aldrich (St. Louis, MO).

2.2. Animal and tissue preparation

Male and female Sprague Dawley rats (250–315 g, Taconic Farms, Germantown, NY) were euthanized with CO_2, and tissues were rapidly removed. Total RNA from brain, liver, kidney, lung, heart and gonads was isolated by Trizol (Invitrogen) and first-strand DNA was synthesized using the First-Strand kit (Invitrogen) according to the manufacturer's instructions.

2.3. Construction of expression plasmids

The full coding region of CYP2C24 was amplified by polymerase chain reaction (PCR) from male rat liver cDNA using the forward primer 5'-ATGGATCCAGTCCTGGTCCT-3' and the reverse primer 5'-TTAACGAGGAATGAAGCACAGC-3'. These primers were designed based on the nucleotide sequence first reported for CYP2C24 cDNA (GenBank accession no. M86677). The reaction mixtures (50 μL) contained 0.2 mM dNTPs, 1 mM $MgSO_4$, 1 U of phusion DNA polymerase (NEB, Ipswich, MA) and each oligonucleotide primer at 0.5 mM. PCR consisted of 35 cycles of denaturation at 98 °C for 10 s, annealing at 65 °C for 10 s and extension at 72 °C for 45 s. The initial denaturation was performed at 98 °C for 30 s. The amplified product (~1500 bp) was purified with a gel extraction kit (Qiagen, Valencia, CA), and the purified PCR products were ligated into pGEM-T (Promega, Madison, WI) and sequenced. The full-length cDNA thus obtained was modified by PCR amplification with 5'-ATGGATCCAGTCCTGGTCCT-3' and 5'-GCTCTAGATTAACGAGGAATGAAGCACAGC-3' as primers under the conditions described above. XbaI was introduced to the 3'-end of the stop codon to facilitate subcloning into the XbaI and EheI of the insect expression vector (pFASTBAC HTA). Three plasmids were constructed for expression and further study: pFASTBAC CYP2C24, pFASTBAC CYP2C24N (His tag on the N-terminal of CYP2C24) and pFASTBAC CYP2C24C (His tag on C-terminal end of CYP2C24). pFASTBAC 2C24 was constructed from 2C24N by inverse PCR using two primers (forward primer 5'-ATGGATCCAGTCCTGGTCCT-3' and the reverse primer 5'-GGTTTCGGACCGAGATCCG-3'). pFASTBAC 2C24C was constructed by adding the His tag through the KpnI and BamHI sites. All plasmids were sequenced.

2.4. Expression of recombinant CYP2C24

The cDNAs coding for CYP2C24 were expressed using a BAC-TO-BAC Baculovirus Expression System (Invitrogen), following the manufacturer's instructions. Recombinant CYP baculoviruses were used to infect Sf9 insect cell cultures in the presence of 0.2 mM hemin. Infected cells were harvested at around 72 h postinfection, the membrane fraction was obtained as described previously[22,23]. In brief, the Sf9 cell pellet was

homogenized (polytron) in 6 volumes of homogenization buffer containing 100 mM Tris-acetate buffer (pH 7.4), 150 mM KCl and 1 mM EDTA. The nuclear fraction and unbroken cells were removed by centrifugation at $100 \times g$ for 10 min at 4 °C. The supernatant fraction was then centrifuged at $100{,}000 \times g$ for 90 min at 4 °C. Pellets were then suspended in membrane storage buffer (50 mM Tris-acetate, pH 7.4, 20% glycerol and 0.1 mM EDTA). CYP2C24 expression levels were determined by CO-difference spectroscopy and Western blot with HisProbe-HRP reagent (Pierce, Rockford, IL).

2.5. Real-time analysis of CYP 2C24 expression

RNA preparation and first-strand DNA synthesis from male and female organs were performed as described above. One μL cDNA was used as the template for each PCR. Primers for real-time PCR of rat CYP2C24 mRNA were forward: 5'-CGCTCATTGCCGATAGTG and reverse: 5'-CGCTTTCCTGTTGAGAAAGG, specifically amplifying a 245 bp fragment of the cDNA. Primers for beta-actin were (forward: 5'-AGGGAAATCGTGCGTGAC and reverse: 5'-CGCTCATTGCCGATAGTG, specifically amplifying a 145 bp fragment of the cDNA. Quantitative real-time PCR was performed using ABsoluteSYBR Green PCR Master Mix according to the manufacturer's instructions (Thermo scientific, USA). Each cDNA sample was analyzed in duplicate. Real-time RT-PCR (25 μL) was performed with 70 nM forward and reverse primers and 1 μL first-strand cDNA template. The program was set at 95 (15 min), followed by 95 °C (20 s) for 45 cycles, 58 °C (20 s) and 72 °C (20 s). Real-time PCR was performed on a MyIQ Single-Color Real-Time PCR Detection System (Bio-Rad, Hercules, CA). CYP 2C24 mRNA levels were calculated using the comparative Ct method and normalized to beta-actin expression levels.

2.6. Measurements of CYP2C24 enzyme activity

Stock concentrations of substrates were dissolved in 100% acetonitrile, with a final concentration of 0.75% (*v*/*v*) in the incubation mixture. Reaction mixtures containing NADPH-regenerating system (0.14 mM $NADP^+$, 0.37 mM D-glucose-6-phosphate, 0.04 U/mL glucose-6-phosphate dehydrogenase, and 0.37 mM magnesium chloride) in 50 mM Tris buffer (pH 7.4) were pre-incubated at 37 °C for 15 min in a total volume of 0.1 mL. Reactions were initiated by the addition (0.1 mL) of CYP2C24 or CYP2C24C, rat P450 oxidoreductase insect control (BD Biosciences, 1 μg) and substrate mixture in Tris buffer (pH 7.4) followed by incubation of a total volume of 0.2 mL at 37 °C. For kinetic studies, fluorescent CYP products were measured in real time with a Victor 3140 Multilabel Counter (Perkin Elmer, Waltham, MA) at 405 nm (excitation) and 460 nm (emission). Incubations for sample blanks used boiled enzyme. Signals from sample blanks were subtracted from all sample values. Product formation was linear for 20 min when using Vivid© BOMCC substrate. Product concentrations were calculated from calibration standard curves of the Vivid© Blue fluorescent standard. Kinetic parameters were calculated by non-linear regression fitting to the Michaels–Menton equation for a single enzyme model using Prism 5.0 software (GraphPad Software Inc., San Diego, CA).

2.7. IC_{50} determinations for CYP2C24

IC_{50} values were estimated according to the method of Crespi et al.[24]. Reaction mixtures containing NADPH-regenerating system were prepared as described above and mixed with inhibitors (from stock concentrations in 100% acetonitrile, diluted to a final concentration of 0.75% acetonitrile). Following pre-incubation at 37 °C for 15 min, reactions were initiated by the addition of CYP2C24C and BOMCC (10 μM final concentration), followed by incubation at 37 °C for 20 min and fluorescent product determination as described above. For time-dependent inhibition studies, inhibitors were pre-incubated in 50 mM Tris (pH 7.4) with enzyme and regenerating system for 0, 15 or 30 min. Substrate was then added, and samples were incubated at 37 °C for an additional 20 min. IC_{50} values were calculated by non-linear regression using the Prism 5.0 sigmoidal dose–response curve function. Statistical analysis of time-dependent inhibition experiments were performed by two-factor analysis of variance (ANOVA, Prism 5.0).

2.8. Measurements of human (CYP2C8, CYP2C9, and CYP2C19) enzyme activities

Human CYP assays (1 pmol per well) were carried out in a total volume of 0.2 mL of 50 mM potassium phosphate buffer (pH 7.4) containing 1% acetonitrile. CYP2C9 activity (1 pmol) was determined with MFC (75 μM) as substrate and incubated at 37 °C for 30 min as described[24]. CYP2C19 and CYP2C8 (both 1 pmol, 0.5 μM DBF) were assayed identically to the method described[25] for CYP2C11. Briefly, inhibitors (in 100% acetonitrile) were added to the reaction mixtures containing NADPH-regenerating system (final concentrations of 1.3 mM $NADP^+$, 3.3 mM D-glucose-6 phosphate, 0.4 U/mL glucose-6-phosphate dehydrogenase, and 3.3 mM magnesium chloride) in 0.1 mL buffer, followed by pre-incubation at 37 °C for 15 min. Reactions were initiated by the addition of 0.1 mL solution containing enzyme and DBF in buffer, incubated at 37 °C for 30 min, and terminated by the addition of 75 μL of 2 M NaOH, followed by a 2 h post incubation at 37 °C. Product formation was determined from a fluorescein standard curve, prepared by spiking fluorescein into the blank incubation mixture. Excitation filter 485 nm (bandwidth 14 nm) and emission filter at 535 nM (bandwidth 25 nm) were used to monitor fluorescein formation.

3. Results

3.1. Expression of CYP2C24 protein in Sf9 cells

The CYP2C24 cDNA was cloned from male liver based on the sequence of the gene[18,19] through a primer polymerase chain reaction strategy. The deduced 490 amino acid sequence was identical with that published previously (GenBank accession No.: P33273) with the exception of Leu→Val substitution at residue 112.

Membrane fractions from Sf9 cells expressing CYP 2C24C were analyzed by reduced CO-difference spectroscopy (Fig. 1, left panel). The spectrum showed the typical Soret peak at 450 nm and a slight peak at 420 nm. No P450 was detected by this method in membrane fractions from control cells or cells

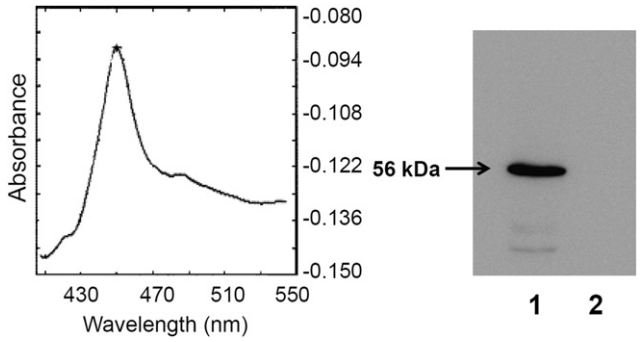

Figure 1 Characteristics of rCYP2C24C. *Left*: Reduced CO-difference spectrum of membrane fraction from Sf9 expressing CYP2C24C. *Right*: Western blot of rCYP2C24C (10 μg protein) was detected by HisProbe-HRP. Lane 1, CYP2C24C; lane 2, Sf9 microsomes infected by wild type baculovirus.

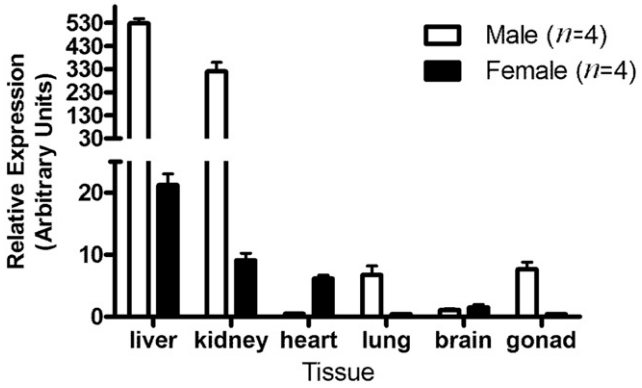

Figure 2 Tissue distribution of CYP2C24 mRNA in male and female adult rats measured by real-time PCR. mRNA levels are expressed as the ratio of CYP2C24 to beta-actin levels in each tissue, normalized to rat male brain (i.e. CYP2C24/β-actin = 1). Each column represents the mean (±SEM) from four measurements.

infected with the wild-type virus (not shown). A Western blot of Sf9 cells expressing CYP 2C24C exhibited a single protein band (lane 1) with an approximate molecular weight of 56.9 kD. No bands were seen from the wild type baculovirus infected Sf9 cells (lane 2). Approximately 70% of the CYP2C24 was found in the membrane fraction, with the remainder in the fraction containing unbroken cells and nuclei. The yield of CYP2C24 from CYP2C24N virus-infected Sf9 cells was much less than that from recombinant CYP2C24C virus-infected Sf9 cells (not shown).

3.2. *Real-time analysis of CYP2C24 expression*

The presence of CYP2C24 mRNA was examined in several rat tissues from both genders. Results (Fig. 2) showed highest CYP2C24 levels in liver and kidney of both sexes, but the enzyme was also detected in brain, lung, heart and gonads. Expression levels were low in brain. In liver, kidney and gonads, CYP2C24 expression was much higher in male than in female rats. This difference was reversed in heart, in which females showed higher expression. Sex differences in CYP2C24 expression were not evident in brain.

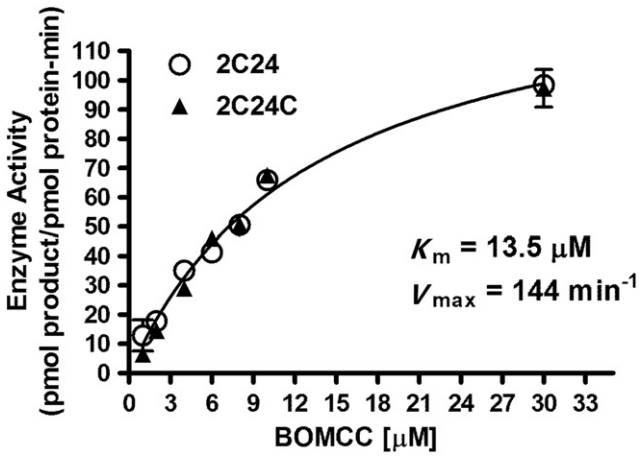

Figure 3 Substrate–velocity curves for the oxidation of BOMCC by CYP2C24 and CYP2C24C. Recombinant enzymes (CYP2C24 and CYP2C2C24C, 20 μg each) isolated from 2000*g* pellets were incubated as described at 37 °C for 20 min. Product formation (ordinate, pmol product/mg enzyme/min) is shown at each concentration of substrate (abscissa). Each data point represents the mean ± SEM of values determined in triplicate. Results for the two enzymes were identical. K_m and V_{max} values, estimated by non-linear regression for the pooled results, are shown.

3.3. *Kinetics of CYP2C24 activity*

In order to develop a high-throughput method for measuring CYP2C24C activity, several known fluorescent substrates for CYP2C enzymes (BOMCC, DBF, 4-BA and C152) were evaluated. Under optimized conditions, BOMCC yielded the highest signal/noise ratio (~6.0 under the conditions described). Using these specified conditions, kinetic studies of CYP2C24 and 2C24C at varying BOMCC concentrations (1–30 μM) were performed (Fig. 3). Fitted kinetic parameters for BOMCC oxidation by CYP2C24 were: $K_m = 13.12 \pm 1.28$ μM and $V_{max} = 141.9 \pm 7.0$ min^{-1}. The K_m and V_{max} values estimated for CYP2C24C were 13.95 ± 1.78 μM and 145.1 ± 9.6 min^{-1}. There were no significant differences in K_m and V_{max} value between CYP2C24 and CYP2C24C.

3.4. *Pharmacological inhibition of CYP2C24*

A variety of CYP inhibitors were studied on CYP2C24C activity (Fig. 4, Table 1). Inhibitory activities ranged from extremely potent (CC12 and MW06-25, IC_{50} values ~25 nM), to moderate (miconazole and sulconazole, ~200 nM), to low (quercetin, sulfaphenazole, fluconazole and ticlopidine, 5–116 μM). The epoxygenase inhibitors MS-PPOH and PPOH were also tested on CYP2C24C (Fig. 5). Concentration–activity curves showed that both drugs had extremely low potencies, with estimated IC_{50} values greater than 300 μM (Fig. 5, Table 1). However, variations in pre-incubation times and the use of very large drug concentrations found time-dependent inhibition by both drugs. For PPOH, a two-factor (concentration, time) ANOVA found significant ($P < 0.001$) main effects for both factors. Fitted PPOH IC_{50} values were 525, 515, and 408 μM, after 0, 15 and 30 min pre-incubation times, respectively. Identical ANOVA results were obtained in the MS-PPOH experiments. Fitted MS-PPOH

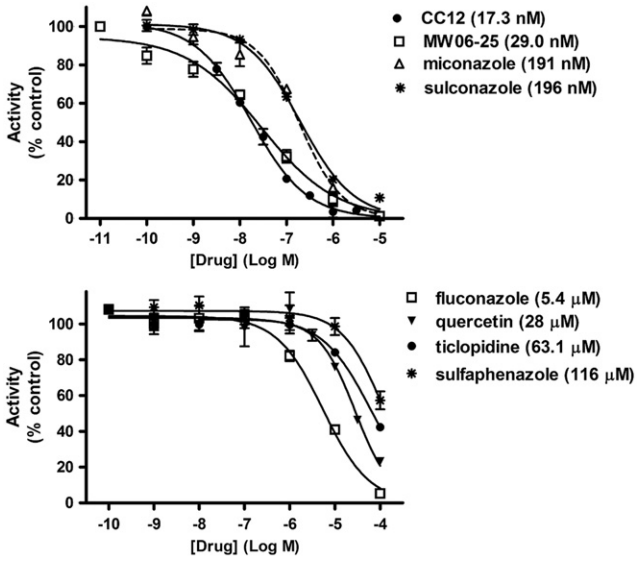

Figure 4 Inhibition of CYP2C24 activity by imidazole-containing drugs. Recombinant CYP2C24 was incubated with substrate and regenerating system in the presence of varying concentrations of inhibitors at 37 °C. Percent control activity (ordinate) is shown at the log of each concentration of inhibitor (abscissa). Each data point represents the mean (±S.E.M.) of 3 determinations. IC_{50} values, estimated by non-linear regression, are given in parentheses and in Table 1.

Table 1 Inhibitor potencies on CYP2C24 and related CYP2C isoforms.

Drug	IC_{50} (μM)			
	CYP2C24[a]	CYP2C8	CYP2C9	CYP2C19
CC12	0.017	2.767[b]	0.059[b]	0.038[c]
MW06-25	0.029	0.566[b]	0.155[b]	0.037[c]
Sulconazole	0.196	0.262[b]	0.02[d]	0.063[b]
Miconazole	0.191	0.442[b]	2.4[d]	0.046[c]
Fluconazole	5.4	>200[e]	19–22[f]	2.959[c]
Quercetin	28	3.50[g]	3.14[h]	6.23[h]
Ticlopidine	63.1	NT	26.4[i]	0.368[i], 4.3[j]
Sulfaphenazole	116.1	NT	0.84[j], 0.29[h]	>500[k]
PPOH	>300	NT	23[l]	300[l]
MS-PPOH	>300	15[m]	11[l]	>80[l]

IC_{50} values for the inhibitors (left) are summarized from current results and relevant literature. NT, not tested.
[a]New results (Figs. 4 and 5).
[b]Unpublished results from this lab (from triplicates).
[c]Conroy et al.[8].
[d]Zhang et al.[44].
[e]Winter and Unadkat[45].
[f]Kunze et al.[46].
[g]Walsky and Gaman[47].
[h]Zou et al.[48].
[i]Ko et al.[49].
[j]Usmani et al.[50].
[k]Marques-Soares et al.[51].
[l]VanAlstine and Hough.[25].
[m]Brand-Schieber et al.[39].

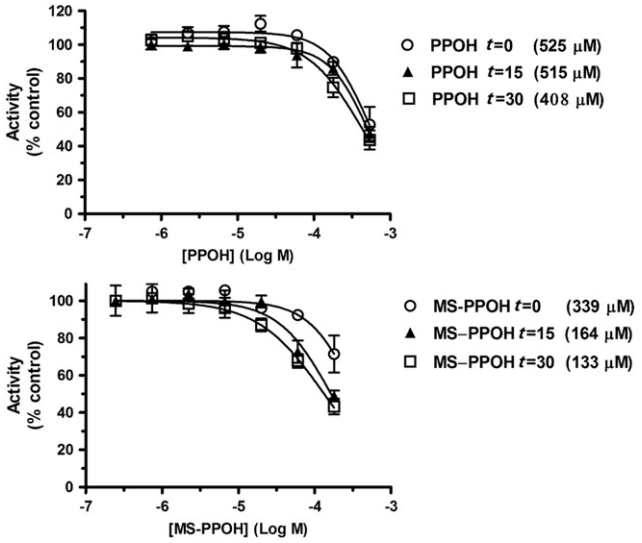

Figure 5 Inhibition of CYP2C24 activity by PPOH (top) and MS-PPOH (bottom). Recombinant CYP2C24 was preincubated with reductase, regenerating system, and the specified concentrations of inhibitors in 50 mM Tris buffer (pH 7.4) at 37 °C. Following the specified preincubation time ($t=0$, 15 or 30 min), samples received substrate (BOMCC, 10 μM) and were incubated at 37 °C for an additional 20 min. Percent control activity (ordinate) is plotted vs. the log of each concentration of inhibitor (abscissa). Each data point represents the mean±S.E.M. of triplicate values. IC_{50} values, estimated by non-linear regression, are given in parentheses for each condition.

IC_{50} values were 339, 164, and 133 μM, at the designated preincubations times.

4. Discussion

CYP2C enzymes comprise the most complex P450 subfamily in humans and rodents. The human group, consisting of four members (CYP2C8, CYP2C9, CYP2C18, and CYP2C19), metabolize endogenous fatty acids[26–28], as well as several clinically-important drugs[17,29–31]. In rats, CYP2Cs constitute approximately 20% of the total liver CYPs[17], but much less is known about the thirteen members of this subfamily (along with CYP2C24, they are CYP2C6, 2C7, 2C11, 2C12, 2C13, 2C22, 2C23, 2C77, 2C79, 2C80, 2C81, and 2C82). Six of these (2C6, 2C7, 2C11, 2C12, 2C13, 2C23) have previously been reported to exist in the brain.[32,16] The present experiments were performed to develop methods to study CYP2C24, to search for its expression in the brain, and to gain specific pharmacological data on this enzyme.

The nucleotide sequence presently cloned from rat liver closely matches that described earlier[18,19], confirming the identity of this product as CYP2C24 (GenBank accession No.: P33273). As expected, this gene encodes a protein of 490 amino acids, and contains the P450 heme-binding signature (FSTGKRMCVG). It should be noted that GenBank identifies this accession number as Cytochrome P450 CYP2C55, with CYP2C24 given as an alternate name. Although CYP2C55 is a recognized isoform in the mouse, expert sources do not use the CYP2C55 name for rat P33273 (e.g. http://drnelson.uthsc.edu/CytochromeP450.html).

Incorporation of His tags into CYP2C24 can streamline the detection and purification of this protein. As mentioned, placement of the His tag on the N-terminal of CYP2C24 dramatically decreased protein expression, as compared with the untagged plasmid. In contrast, incorporation of the His tag on the C-terminal did not change expression levels or enzyme activity (Fig. 4). These findings suggest that the hydrophobic N-terminal segment may be important for the proper folding and assembly of this CYP. This conclusion apparently does not apply to all CYPs, since the addition of a His tag to the N-terminal of CYP2C2 increased protein expression[33]. Holla et al.[20] used the baculovirus/sf9 system for the heterologous expression of CYP2C11, CYP 2C23 and CYP2C24. These authors did not incorporate His tags into any of the plasmids, but did note much lower expression levels for CYP2C24 as compared with the other two enzymes. The presently-demonstrated expression and activity of CYP2C24C show this plasmid to be useful for additional purification and study of this enzyme.

The present detection of CYP2C24 mRNA in male rat liver and kidney (Fig. 2) confirms an earlier Northern analysis[18]. This study identified CYP2C24 mRNA in male, but not female, adult kidney, consistent with a 30-fold higher level in male kidney seen presently. The same paper[18] found no such sex difference in liver expression of this mRNA, in stark contrast with the present results. Gender differences in expression levels of other CYP2C enzymes are well known, with the best examples being the male-specific CYP2C11, CYP2C13, and CYP3A2, and the female-specific CYP2C12[34]. The existence of CYP2C24 mRNA in lung, heart, gonad and brain (Fig. 2) has not been previously reported. These findings suggest the possibility that this enzyme has functional significance in the brain and/or other organs studied. A reverse gender difference (i.e. female greater than male) in CYP2C24 levels in the heart (Fig. 2) has also not been reported previously, and requires further study.

In vitro studies of CYP activity have often been hampered by low enzyme activity, poor solubility of substrates and sometimes high background fluorescence[35]. In the only prior study of CYP2C24 activity, measurements of AA epoxidation by this enzyme showed very low activity[20]; such a reaction cannot presently be monitored by high-throughput methods. Our results, showing that CYP2C24 activity can be efficiently measured by use of the Vivid© BOMCC reagent in 96-well plates, demonstrate a reliable, high-throughput method for studying this enzyme. This substrate has been used successfully to measure the activity of CYP2C19[35] and several other CYP isoforms (see http://www.invitrogen.com.cn/downloads/O-13873-r1_US_0405.pdf).

Pharmacological characterization of CYP2C24 could ultimately help to understand its biological significance. The list of inhibitors studied presently (Table 1) includes drugs with reported selectivity towards CYP2C9 (sulfaphenazole), 2C19 (ticlopidine, fluconazole), and CYP2C8 (quercetin), as well as less selective inhibitors. The CYP epoxygenase inhibitors (PPOH and MS-PPOH) were also studied. Finally, the list also includes CC12 and MW06-25, two imidazole-containing CYP inhibitors found to block analgesic activity in the brain[8,36]. Activities on CYP2C24 were compared (Table 1) and correlated (Fig. 6) with relative activities on three other CYP2C isoforms. Although it is recognized that inhibitor K_i (vs. IC_{50}) values would be most valuable in making comparisons across enzymes, many of the studies cited in Table 1 did not report information sufficient for K_i calculations. Furthermore, the mechanisms of action of most of these inhibitors are not known.

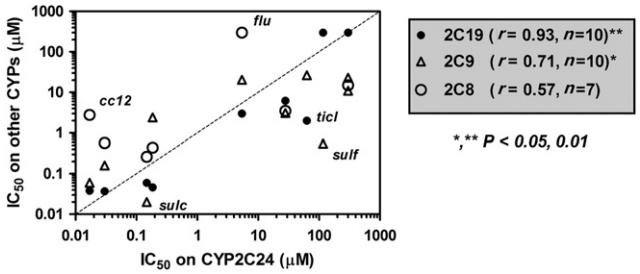

Figure 6 Correlations between inhibitor potencies on CYP2C24 and potencies on human CYP2C isoforms. IC_{50} values for ten inhibitors on CYP2C24 are plotted (abscissa, log scale) against IC_{50} values for the same drugs determined CYP2C19, CYP2C9, and CYP2C8 (ordinate, log scale). For each pair of CYPs plotted, values were analyzed by the Spearman rank correlation test. Dashed line indicates the theoretical perfect correlation. Outliers in each correlation are identified by drug abbreviation (*sulc*, sulconazole; *flu*, fluconazole; *ticl*, ticlopidine, *sulf*, sulfaphenazole). For example, a near-perfect correlation was observed between potencies on CYP2C24 vs. potencies on CYP2C19 except for *ticl*, which is approximately 30-fold less potent on CYP2C24. All data are from Table 1. Mean values are plotted when the table gave more than one value. For plotting and correlational analyses, values in the table estimated to be larger than 200 μM were arbitrarily designated as 300 μM.

Activity of the compounds on CYP2C24 was very highly correlated with activity on CYP2C19 (Fig. 6, $r=0.93$, $P<0.01$). These findings, showing strong pharmacological similarities between the enzymes, are consistent with their high sequence homologies (74%), and confirm that rat CYP2C24 closely resembles human CYP2C19. Notable similarities in inhibitor actions include CC12 and MW06-25 (very potent on both), and PPPOH (very low activity on both, further discussed below). CC12 is not a selective CYP2C24/CYP2C19 inhibitor, since it was shown to block 16 human CYPs in the 12–500 nM concentration range[37]. MW06-25 may have more selectivity, but less is known about the CYP inhibitory profile of this compound[8]. The single outlier in the CYP2C24–CYP2C19 correlation was ticlopidine, which was 16–160-fold less active on CYP2C24. Inhibition of CYP2C24 was also significantly correlated with activity on CYP2C9 (Fig. 6, $r=0.71$, $P<0.05$). Notable outliers in this correlation were sulfaphenazole and sulconazole, which were much less active on CYP2C24 as compared with CYP2C9. Among the enzymes studied, the inhibitor profile on CYP2C24 was least correlated with the activity on CYP2C8. CC12 and fluconazole were considerably less potent on CYP2C8 than predicted from their actions on CYP2C24. Taken together, these results show that CYP2C24 has a CYP2C-like profile, but no highly selective inhibitors of this enzyme were identified.

The acetylenic fatty acid derivatives PPOH and MS-PPOH were initially characterized as selective inhibitors of AA epoxygenase (vs. AA hydroxylase) in renal cortical microsomes[38,39]. Best known CYP epoxygenase targets for one or both of these drugs are CYP4A2, CYP4A3[40], and CYP2C8[39]. PPOH and MS-PPOH have been used extensively in CYP epoxygenase research,

and, although these drugs have been widely assumed to be general inhibitors of all CYP epoxygenases, a recent study found this to not be the case[25]. Predictably, PPOH was found to be a potent inhibitor of the epoxygenases CYP2B1 and CYP2C9, but only a moderate inhibitor of CYP2B6 and CYP2C11. Surprisingly, however, this drug only weakly inhibited the epoxygenases CYP2C6 and CYP2C19[25] (see also Table 1). As compared with PPOH, MS-PPOH inhibited even fewer epoxygenases, with only very weak activity on CYP2B6[25]. Since CYP2C24 was previously reported to have AA epoxygenase activity[20], it was of interest to assess the inhibitory activity of these drugs on CYP2C24. The present results, showing very low activity of PPOH and MS-PPOH on CYP2C24, provide additional similarities between this enzyme and CYP2C19 (Table 1). Furthermore, these findings support the conclusion[25] that PPOH and MS-PPOH do not inhibit all CYP epoxygenases.

Terminal acetylenic fatty acids (such as PPOH and MS-PPOH) have been proposed to function as ''suicide substrates'', also known as mechanism-based inhibitors[41]. Such compounds are presumed to undergo enzymatic oxidation, followed by enzyme inactivation, producing a long-acting, irreversible inhibition of activity. It is important to establish whether these compounds act by such a mechanism, since these drugs may act at both CYP and non-CYP targets[42]. A mechanism-based action, if verified, would only be expected on the CYP targets. Our lab[25] recently reported time- and NADPH-dependent inhibition of CYP2C6, CYP2C9 CYP2C11, and CYP2B1 by PPOH and MS-PPOH, consistent with mechanism-based inhibition of these enzymes. Although the present results found these drugs to be very weak inhibitors of CYP2C24, the time-dependent inhibition of this enzyme by both PPOH and MS-PPOH (Fig. 5), is consistent with this mechanism.

Our laboratory became interested in brain CYPs through studies of the CNS pain-relieving properties of the histamine H_2 receptor antagonist cimetidine, and its non-H_2-acting congener improgan[43]. Searching for the analgesic targets of these drugs, we characterized in detail the high affinity binding of ^{3}H-cimetidine (^{3}H-CIM) in rat brain homogenates[37]. High affinity ^{3}H-CIM binding in brain was unrelated to the histamine H_2 receptor, but showed strong biochemical similarities to a heme-containing CYP protein. Potent inhibition of the binding by the CYP2C19 inhibitor tranylcypromine suggested that the rat brain ^{3}H-CIM-binding protein(s) resemble human CYP2C19. However, ^{3}H-CIM did not bind to recombinant CYP2C19, to seven other human CYPS, or to three rat CYPs (2B1, 2C6, and 2C11)[37]. The authors concluded that ^{3}H-CIM binds to one or more unidentified CYP proteins in the rat brain[37]. Since the pharmacology of ^{3}H-CIM binding in rat brain resembles that of human CYP2C19, the similarities between CYP2C24 and CYP2C19 (Fig. 6) suggested the possibility that brain CYP2C24 accounted for ^{3}H-CIM in the rat brain. However, the present results do not support this hypothesis, since ticlopidine, sulfaphenazole and quercetin (all inhibitors of CYP2C24, Table 1) were completely inactive on the rat brain binding at 100 μM[37]. Furthermore, unpublished studies in our lab did not detect ^{3}H-CIM binding in preparations of CYP2C24C when tested as described[37]. Thus, the ^{3}H-CIM-binding protein in rat brain (likely to be a CYP) remains to be identified.

Recent studies from our laboratory used transgenic and pharmacological approaches to show that one or more brain CYPs is essential in signal transduction pathways following administration of either opioid[8] or non-opioid (i.e. improgan)[36] analgesic drugs. Support for the hypothesis that these analgesic drugs (acting through difference receptors) activate pain-relieving circuits through stimulation of AA epoxidation has been summarized[8,36]. The findings include inhibition of analgesia by general CYP inhibitors and by MS-PPOH, but studies to date have not identified the relevant CYP epoxygenase(s). The present pharmacological characterization of CYP2C24 (Table 1) is useful for assessing the importance of this enzyme for analgesic mechanisms. For improgan analgesia, detailed *in vivo* dose–response curves show a rank order of inhibitory activity (most to least potent) to be MS-PPOH > fluconazole > miconazole > MW06-25 > CC12[36]. Since Table 1 shows nearly the exact opposite potency rank for these compounds acting on CYP2C24, the present findings make highly unlikely that this brain enzyme contributes to improgan analgesia. *In vivo* pharmacological data on inhibition of opioid analgesia is much less complete, but ongoing and published studies[8,21] suggest a probable rank order of inhibitory activity against morphine action to be MW06-25 > MS-PPOH > CC12, also distinct from Table 1. These results suggest that CYP2C24 is unlikely to participate in CNS analgesic drug action. Additional studies to identify the biological significance of CYP2C24 will be facilitated by our present findings on the tissue distribution and pharmacological inhibition of this enzyme.

Acknowledgments

We thank Drs. Qingyu Zhang and Xin Zhou of the Wadsworth Center, New York State Department of Health (Albany, NY) for assistance with biochemical characterization of CYP2C24. We also thank Julia W. Nalwalk for helpful comments on the manuscript. This work was supported by grants from the National Institute on Drug Abuse (DA-03814 and DA-027835).

References

1. Capdevila JH, Falck JR, Estabrook RW. Cytochrome P450 and the arachidonate cascade. *FASEB J* 1992;**6**:731–6.
2. Capdevila JH, Dishman E, Karara A, Falck JR. Cytochrome P450 arachidonic acid epoxygenase: stereochemical characterization of epoxyeicosatrienoic acids. *Methods Enzymol* 1991;**206**: 441–53.
3. Kroetz DL, Zeldin DC. Cytochrome P450 pathways of arachidonic acid metabolism. *Curr Opin Lipidol* 2002;**13**:273–83.
4. Pfister SL, Gauthier KM, Campbell WB. Vascular pharmacology of epoxyeicosatrienoic acids. *Adv Pharmacol* 2010;**60**:27–59.
5. Sudhahar V, Shaw S, Imig JD. Epoxyeicosatrienoic acid analogs and vascular function. *Curr Med Chem* 2010;**17**:1181–90.
6. Iliff JJ, Wang R, Zeldin DC, Alkayed NJ. Epoxyeicosanoids as mediators of neurogenic vasodilation in cerebral vessels. *Am J Physiol Heart Circ Physiol* 2009;**296**:H1352–63.
7. Heinricher MM, Maire JJ, Lee D, Nalwalk JW, Hough LB. Physiological basis for inhibition of morphine and improgan antinociception by CC12, a P450 epoxygenase inhibitor. *J Neurophysiol* 2010;**104**:3222–30.
8. Conroy JL, Fang C, Gu J, Zeitlin SO, Yang W, Yang J, et al. Opioids activate brain analgesic circuits through cytochrome P450/epoxygenase signaling. *Nat Neurosci* 2010;**13**:284–6.

9. Terashvili M, Tseng LF, Wu HE, Narayanan J, Hart LM, Falck JR, et al. Antinociception produced by 14,15-epoxyeicosatrienoic acid is mediated by the activation of beta-endorphin and met-enkephalin in the rat ventrolateral periaqueductal gray. *J Pharmacol Exp Ther* 2008;**326**:614–22.
10. Capdevila JH, Falck JR, Harris RC. Cytochrome P450 and arachidonic acid bioactivation. Molecular and functional properties of the arachidonate monooxygenase. *J Lipid Res* 2000;**41**: 163–81.
11. Zeldin DC. Epoxygenase pathways of arachidonic acid metabolism. *J Biol Chem* 2001;**276**:36059–62.
12. Imig JD. Epoxygenase metabolites. Epithelial and vascular actions. *Mol Biotechnol* 2000;**16**:233–51.
13. Thompson CM, Capdevila JH, Strobel HW. Recombinant cytochrome P450 2D18 metabolism of dopamine and arachidonic acid. *J Pharmacol Exp Ther* 2000;**294**:1120–30.
14. Oleksiak MF, Wu S, Parker C, Karchner SI, Stegeman JJ, Zeldin DC. Identification, functional characterization, and regulation of a new cytochrome P450 subfamily, the CYP2Ns. *J Biol Chem* 2000;**275**:2312–21.
15. Stark K, Dostalek M, Guengerich FP. Expression and purification of orphan cytochrome P450 4X1 and oxidation of anandamide. *FEBS J* 2008;**275**:3706–17.
16. Iliff JJ, Jia J, Nelson J, Goyagi T, Klaus J, Alkayed NJ. Epoxyeicosanoid signaling in CNS function and disease. *Prostaglandins Other Lipid Mediat* 2009;**91**:68–84.
17. Martignoni M, Groothuis GM, de Kanter R. Species differences between mouse, rat, dog, monkey and human CYP-mediated drug metabolism, inhibition and induction. *Expert Opin Drug Metab Toxicol* 2006;**2**:875–94.
18. Zaphiropoulos PG. cDNA cloning and regulation of a novel rat cytochrome P450 of the 2C gene subfamily (P450IIC24). *Biochem Biophys Res Commun* 1991;**180**:645–51.
19. Zaphiropoulos PG. Differential expression of cytochrome P450 2C24 transcripts in rat kidney and prostate: evidence indicative of alternative and possibly trans splicing events. *Biochem Biophys Res Commun* 1993;**192**:778–86.
20. Holla VR, Makita K, Zaphiropoulos PG, Capdevila JH. The kidney cytochrome P-450 2C23 arachidonic acid epoxygenase is upregulated during dietary salt loading. *J Clin Invest* 1999;**104**: 751–60.
21. Hough LB, Nalwalk JW, Phillips JG, Kern B, Shan Z, Wentland MP, et al. CC12, a high-affinity ligand for [^{3}H] cimetidine binding, is an improgan antagonist. *Neuropharmacology* 2007;**52**: 1244–55.
22. Ding XX, Coon MJ. Purification and characterization of two unique forms of cytochrome P-450 from rabbit nasal microsomes. *Biochemistry* 1988;**27**:8330–7.
23. Trogadis JE, Ng GY, O'Dowd BF, George SR, Stevens JK. Dopamine D1 receptor distribution in Sf9 cells imaged by confocal microscopy: a quantitative evaluation. *J Histochem Cytochem* 1995;**43**:497–506.
24. Crespi CL, Miller VP, Penman BW. Microtiter plate assays for inhibition of human, drug-metabolizing cytochromes P450. *Anal Biochem* 1997;**248**:188–90.
25. VanAlstine MA, Hough LB. Effects of acetylenic epoxygenase inhibitors on recombinant cytochrome P450s. *Drug Metab Dispos* 2011;**39**:1221–6.
26. Daikh BE, Lasker JM, Raucy JL, Koop DR. Regio- and stereoselective epoxidation of arachidonic acid by human cytochromes P450 2C8 and 2C9. *J Pharmacol Exp Ther* 1994;**271**: 1427–33.
27. Bylund J, Ericsson J, Oliw EH. Analysis of cytochrome P450 metabolites of arachidonic and linoleic acids by liquid chromatography-mass spectrometry with ion trap MS. *Anal Biochem* 1998;**265**:55–68.
28. Zeldin DC, DuBois RN, Falck JR, Capdevila JH. Molecular cloning, expression and characterization of an endogenous human cytochrome P450 arachidonic acid epoxygenase isoform. *Arch Biochem Biophys* 1995;**322**:76–86.
29. Goldstein JA, de Morais SM. Biochemistry and molecular biology of the human CYP2C subfamily. *Pharmacogenetics* 1994;**4**:285–99.
30. Rahman A, Korzekwa KR, Grogan J, Gonzalez FJ, Harris JW. Selective biotransformation of taxol to 6 alpha-hydroxytaxol by human cytochrome P450 2C8. *Cancer Res* 1994;**54**:5543–6.
31. Andersson T, Regardh CG, Lou YC, Zhang Y, Dahl ML, Bertilsson L. Polymorphic hydroxylation of S-mephenytoin and omeprazole metabolism in Caucasian and Chinese subjects. *Pharmacogenetics* 1992;**2**:25–31.
32. Hedlund E, Gustafsson JA, Warner M. Cytochrome P450 in the brain; a review. *Curr Drug Metab* 2001;**2**:245–63.
33. Doray B, Chen CD, Kemper B. N-terminal deletions and His-tag fusions dramatically affect expression of cytochrome p450 2C2 in bacteria. *Arch Biochem Biophys* 2001;**393**:143–53.
34. Czerniak R. Gender-based differences in pharmacokinetics in laboratory animal models. *Int J Toxicol* 2001;**20**:161–3.
35. Trubetskoy OV, Gibson JR, Marks BD. Highly miniaturized formats for *in vitro* drug metabolism assays using vivid fluorescent substrates and recombinant human cytochrome P450 enzymes. *J Biomol Screen* 2005;**10**:56–66.
36. Hough LB, Nalwalk JW, Yang J, Conroy JL, VanAlstine MA, Yang W, et al. Brain P450 epoxygenase activity is required for the antinociceptive effects of improgan, a nonopioid analgesic. *Pain* 2011;**152**:878–87.
37. Stadel R, Yang J, Nalwalk JW, Phillips JG, Hough LB. High-affinity binding of [^{3}H]cimetidine to a heme-containing protein in rat brain. *Drug Metab Dispos* 2008;**36**:614–21.
38. Wang MH, Brand-Schieber E, Zand BA, Nguyen X, Falck JR, Balu N, et al. Cytochrome P450-derived arachidonic acid metabolism in the rat kidney: characterization of selective inhibitors. *J Pharmacol Exp Ther* 1998;**284**:966–73.
39. Brand-Schieber E, Falck JF, Schwartzman M. Selective inhibition of arachidonic acid epoxidation *in vivo*. *J Physiol Pharmacol* 2000;**51**:655–72.
40. Nguyen X, Wang MH, Reddy KM, Falck JR, Schwartzman ML. Kinetic profile of the rat CYP4A isoforms: arachidonic acid metabolism and isoform-specific inhibitors. *Am J Physiol* 1999;**276**: R1691–700.
41. Zou AP, Ma YH, Sui ZH, Ortiz de Montellano PR, Clark JE, Masters BS, et al. Effects of 17-octadecynoic acid, a suicide-substrate inhibitor of cytochrome P450 fatty acid omega-hydroxylase, on renal function in rats. *J Pharmacol Exp Ther* 1994;**268**: 474–81.
42. Chen Y, Falck JR, Tuniki VR, Campbell WB. 20-^{125}Iodo-14,15-epoxyeicosa-5(*Z*)-enoic acid: a high-affinity radioligand used to characterize the epoxyeicosatrienoic acid antagonist binding site. *J Pharmacol Exp Ther* 2009;**331**:1137–45.
43. Hough LB, Nalwalk JW, Barnes WG, Leurs R, Menge WM, Timmerman H. A third legacy for burimamide: discovery and characterization of improgan and a new class of non-opioid analgesics derived from histamine antagonists. Watanabe T, Timmerman H, Yanai K, editors. *Excerpta medica international congress series 1224*. Proceedings of the international Sendai histamine symposium: histamine research in the new millenium; 2000 November; Sendai, Japan. Amsterdam: Elsevier; 2001. p. 237–42.
44. Zhang W, Ramamoorthy Y, Kilicarslan T, Nolte H, Tyndale RF, Sellers EM. Inhibition of cytochromes P450 by antifungal imidazole derivatives. *Drug Metab Dispos* 2002;**30**:314–8.
45. Winter HR, Unadkat JD. Identification of cytochrome P450 and arylamine *N*-acetyltransferase isoforms involved in sulfadiazine metabolism. *Drug Metab Dispos* 2005;**33**:969–76.
46. Kunze KL, Wienkers LC, Thummel KE, Trager WF, Warfarin-fluconazole. I. Inhibition of the human cytochrome P450-dependent metabolism of warfarin by fluconazole: *in vitro* studies. *Drug Metab Dispos* 1996;**24**:414–21.

47. Walsky RL, Gaman EA, Obach RS. Examination of 209 drugs for inhibition of cytochrome P450 2C8. *J Clin Pharmacol* 2005;**45**: 68–78.
48. Zou L, Harkey MR, Henderson GL. Effects of herbal components on cDNA-expressed cytochrome P450 enzyme catalytic activity. *Life Sci* 2002;**71**:1579–89.
49. Ko JW, Desta Z, Soukhova NV, Tracy T, Flockhart DA. *In vitro* inhibition of the cytochrome P450 (CYP450) system by the antiplatelet drug ticlopidine: potent effect on CYP2C19 and CYP2D6. *Br J Clin Pharmacol* 2000;**49**:343–51.
50. Usmani KA, Karoly ED, Hodgson E, Rose RL. *In vitro* sulfoxidation of thioether compounds by human cytochrome P450 and flavin-containing monooxygenase isoforms with particular reference to the CYP2C subfamily. *Drug Metab Dispos* 2004;**32**:333–9.
51. Marques-Soares C, Dijols S, Macherey AC, Wester MR, Johnson EF, Dansette PM, et al. Sulfaphenazole derivatives as tools for comparing cytochrome P450 2C5 and human cytochromes P450 2Cs: identification of a new high affinity substrate common to those enzymes. *Biochemistry* 2003;**42**:6363–9.